MicroRNA-132 mediates proliferation and migration of pulmonary smooth muscle cells via targeting PTEN

ZHEN-HUA ZENG[1*], WEI-HUA WU[2*], QI PENG[2], YA-HUI SUN[2] and JIAN-XIN LIU[2]

[1]Hunan Province Key Laboratory for Antibody-based Drug and Intelligent Delivery System Biomedical Research Center, Hunan University of Medicine; [2]Department of Pharmacology, School of Pharmaceutical Sciences, Hunan University of Medicine, Huaihua, Hunan 418000, P.R. China

Received September 15, 2018; Accepted March 8, 2019

DOI: 10.3892/mmr.2019.10053

Abstract. Pulmonary arterial hypertension (PAH) is a severe and progressive disease characterized by the remodeling of small pulmonary arteries. The aberrant proliferation of pulmonary arterial smooth muscle cells (PASMCs) is the primary feature of PAH. MicroRNA (miR)-132 has been demonstrated to inhibit the proliferation of vascular smooth muscle cells and repress neointimal formation. Phosphatase and tensin homolog deleted on chromosome 10 (PTEN) is a direct target of miR-132 that has been revealed to be involved in the development of PAH. However, the role of miR-132 in PAH remains unclear. The present study demonstrated that miR-132 expression was upregulated in monocrotaline-induced PAH rats and platelet-derived growth factor-induced PASMCs. In addition, treatment of PASMCs with miR-132 mimics inhibited their proliferation, whereas miR-132 inhibition exhibited the opposite effects. Furthermore, miR-132 mimics promoted cell migration and maintained the PASMC contractile phenotype. Finally, the expression levels of PTEN were significantly decreased in PAH and PASMCs treated with miR-132 mimics. Taken collectively, the data suggested that miR-132 regulated PASMC function via PTEN and that it may be used as a potential target for the treatment of PAH.

Introduction

Pulmonary arterial hypertension (PAH) is a chronic severe disease characterized by the obliteration of small pulmonary arteries (Pas) and progressive development of pulmonary vascular resistance, which eventually leads to right heart failure and mortality (1). In PAH, the aberrant growth, migration and phenotypic switch of pulmonary arterial smooth muscle cells (PASMCs) serve a vital role in the vascular remodeling and constriction of distal Pas (2). Therefore, the inhibition of PASMC proliferation, migration and phenotypical alteration is a prospective strategy for the treatment of PAH.

In addition to genetic, epigenetic and environmental factors, the function of PASMCs is affected by numerous endogenous molecules, including platelet-derived growth factor BB (PDGF-BB), transforming growth factor-β and fibroblast growth factor (FGF) (3,4). It has been demonstrated that PDGF-BB may affect PASMC function via the regulation of the downstream signals required for the progression of PAH (5). In addition, previous studies demonstrated that the regulation of several microRNAs (miRNAs/miR) by PDGF-BB was critical for PASMC function (6,7).

miRNAs are small endogenous non-coding RNAs that serve as repressors of gene expression by regulating the stability of their target mRNAs (8). It is well-known that miRNAs are involved in the pathological processes of PAH (9,10). Several of these miRNAs, including miR-204 (11), miR-214 (12), let-7g (13), miR-143/145 (14), mir-130/301 (15) and miR-135a-5p (16) regulate PASMC function.

Previous studies have suggested that miR-132 inhibited vascular smooth muscle cell (VSMC) proliferation and repressed neointimal formation (17). Furthermore, phosphatase and tensin homolog deleted on chromosome 10 (PTEN) is a direct target of miR-132 (18) and is involved in the development of PAH (19). However, the exact mechanism of this interaction remains unclear. Therefore, the present study aimed to identify the role of miR-132 in the development of PAH *in vivo* and *in vitro*.

In the present study, it was demonstrated that miR-132 was upregulated in the monocrotaline (MCT)-induced PAH rats and PDGF-BB-treated PASMCs. The results additionally revealed that miR-132 may affect the proliferation, migration and phenotypic switching of PASMCs via the PTEN signaling pathway.

Materials and methods

Experimental animal model and treatment. A total of 16 Sprague-Dawley male rats (~11 weeks old, 180-200 g) were

Correspondence to: Professor Wei-Hua Wu, Department of Pharmacology, School of Pharmaceutical Sciences, Hunan University of Medicine, 492 South Jinxi Street, Huaihua, Hunan 418000, P.R. China
E-mail: wwh815@hotmail.com

*Contributed equally

Key words: microRNA-132, pulmonary arterial hypertension, smooth muscle cell, proliferation, phenotypic switching

obtained from the Hunan Slack Jingda Laboratory Animal Co., Ltd. (Changsha, China). The rats was subjected to controlled conditions of 20-22˚C, relative humidity of 50-55% and a 12-h light/dark cycle, and provided with *ad libitum* access to food and water. The experiments were performed in accordance with the National Institutes of Health guidelines for the care and use of laboratory animals (20) and were approved by the Ethics Committee of the Hunan University of Medicine (Huaihua, China). The rats received a subcutaneous injection of 60 mg/kg MCT (Sigma-Aldrich; Merck KGaA, Darmstadt, Germany) for the induction of PAH. Control rats received 0.9% saline.

Hemodynamic measurements. PAH was established in the rats by the 21st day following injection, at which point the rats were anesthetized via an intraperitoneal injection of 60 mg/kg pentobarbital sodium. A jugular catheter (1 mm) filled with heparinized saline was introduced into the right external jugular vein, and subsequently advanced through the right atrium and right ventricle (RV). Appropriate positioning of the catheter was confirmed by the change of the pressure waveform. Once the change in the pressure waveform was stable, the RV systolic pressure (RVSP) was measured with a multichannel physiological recorder monitoring equipment (BL-420F).

Hematoxylin and eosin (H&E) staining. The rats were immediately sacrificed by cervical dislocation following the hemodynamic measurements. Sacrifice was confirmed by a lack of breathing and blood pressure, following which lung tissues were quickly harvested and fixed in 4% paraformaldehyde at 4˚C for 24 h. The paraffin-embedded lung tissue samples were cut into 4-μm thick sections and stained with 0.1% Mayer's hematoxylin (Sigma-Aldrich; Merck KGaA) for 5 min and 0.5% eosin Y solution (Sigma-Aldrich; Merck KGaA) for 40 sec at room temperature. Structural changes in the pulmonary vascular wall and the wall thickness were observed using a Zeiss Axio Scope.A1 microscope (magnification, x200; Zeiss GmbH, Jena, Germany). Between six to eight vessels were analyzed per animal, and four values for the thickness and two values for the diameter were measured for each vessel. Percentage wall thickness (wall thickness/vessel diameter) was calculated.

Cell culture and treatment. Human PASMCs were obtained from PromoCell GmbH (Heidelberg, Germany) and were maintained in smooth muscle cell growth medium (SMCGM; PromoCell GmbH) containing 5% fetal bovine serum (FBS; Gibco; Thermo Fisher Scientific, Inc., Waltham, MA, USA) and 1% penicillin/streptomycin (Gibco; Thermo Fisher Scientific, Inc.). Human PASMCs were starved in SMCGM containing a low percentage of serum (0.2% FBS) for 24 h prior to treatment with PDGF-BB (Sangon Biotech Co., Ltd., Shanghai, China) at 37˚C. Cells were treated with various concentrations of PDGF-BB (5, 10, 20, 40 and 80 ng/ml) for 24 h, or with 20 ng/ml PDGF-BB for various incubation periods (2, 6, 12, 24 and 48 h). RNA was extracted from PAMSCs following treatment, as described below. Each independent experiment was performed at least 3 times.

miRNA transfection. The miR-132 mimics (miR10000426), the miR-132 inhibitors (miR20000426), the mimic negative control (NC; miR1N0000001) and inhibitor NC (miR2N0000001) were purchased from Guangzhou RiboBio Co., Ltd., (Guangzhou, China). The mimics and inhibitors were synthesized on the basis of sequence of hsa-miR-132-3p (5'-UAACAGUCUACAGCCAUGGUC G-3'). Human PASMCs were seeded in 6-well culture plates at a density of $2x10^5$ cells/well, incubated for 24 h, and transfected with miR-132 mimics (20 nM), miR-132 inhibitor (50 nM) or NCs (20 nM for mimics; 50 nM for inhibitors) for 6 h according to the instructions provided by the manufacturer of the Hiperfect Transfection Reagent (Qiagen GmbH, Hilden, Germany). The culture media was replaced and the cells were further incubated for 42-66 h prior to subsequent experiments.

Cell proliferation assay. PASMCs were seeded in a 96-well plate. Cell viability was determined with an MTS CellTiter 96® AQ_{ueous} one solution cell proliferation assay (Promega Corporation, Madison, WI, USA). The absorbance was detected by spectrophotometry at 490 nM using a Berthold LB-942 instrument (Berthold Technologies GmbH & Co., KG, Bad Wildbad, Germany).

Cell cycle analysis. PASMCs were treated in groups as indicated in the transfection protocol and fixed with 70% ethanol overnight at 4˚C. Following washing with cold PBS, 5 μl RNase A (10 mg/ml) was added to the cells. Subsequently, the cells were stained with 1 mg/ml propidium iodide solution (Sigma-Aldrich; Merck KGaA) for 15 min at 4˚C. The cell cycle analysis was performed by flow cytometry (CytoFLEX; Beckman Coulter, Inc., Brea, CA, USA) and the results were analyzed using ModFit LT 3.3 software (Verity Software House, Inc., Topsham, ME, USA).

Transwell assay. Cell migration was assessed using a Transwell assay. The transfected cells were seeded in the top chamber containing medium with 0.1% FBS. The lower chamber was filled with SMCGM containing 5% FBS. PASMCs were allowed to migrate for 24 h at 37˚C. The cells were fixed in 4% paraformaldehyde for 30 min and then stained with 0.1% crystal violet for 30 min, each at room temperature. Finally, the cells from five random fields were counted using a Zeiss Axio Vert.A1 microscope (magnification, x200; Zeiss GmbH) and the images were processed using Image-Pro Plus 6.0 software (Media Cybernetics, Inc., Rockville, MD, USA).

RNA preparation and reverse transcription quantitative polymerase chain reaction (RT-qPCR) analysis. The total RNA of PASMCs and lung tissues was extracted using TRIzol® reagent (Thermo Fisher Scientific, Inc.) as described previously (21). The concentration of the RNA samples was quantified using NanoDrop One spectrophotometer (NanoDrop Technologies; Thermo Fisher Scientific, Inc., Wilmington, DE, USA). Purified RNA was reverse transcribed with PrimeScript™ RT reagent (Takara Bio, Inc., Otsu, Japan) at 37˚C for 15 min and 85˚C for 5 sec. Mature miRNA was reverse transcribed with Bulge-Loop™ miRNA qPCR primers (Guangzhou RiboBio Co., Ltd.) prior to qPCR according to the manufacturer's protocol. The qPCR experiments were conducted using an SYBR Premix ExTaq™

kit (Takara Biotechnology, Co., Ltd., Dalian, China) in a LightCycler 480 Real-Time PCR System (Roche Applied Science, Mannheim, Germany). PCR was conducted as follows: 95˚C for 30 sec, followed by 40 cycles of 95˚C for 5 sec and 60˚C for 30 sec. The expression levels were quantified using the $2^{-\Delta\Delta Cq}$ method (22) with *U6* and *β-actin* as the endogenous reference genes for miRNA and mRNA expressions, respectively. The primer sequences were as follows: α-smooth muscle actin (*α-SMA*) forward, 5'-TATCAGGGG GCACCACTATG-3' and reverse, 5'-AGGAGCAGGAAA GTGTTTTAGA-3'; transgelin (*SM22α*) forward, 5'-TGG TGAACAGCCTGTACCCT-3' and reverse, 5'-CACGGTAGT GCCCATCATTC-3'; calponin 1 (*CNN1*) forward, 5'-TGC TACAGGGTCCAACATAGA-3' and reverse, 5'-GTTGCT CAGTGCGTCCTT-3'; *β-actin* forward, 5'-TGTCACCAA CTGGGACGATA-3' and reverse, 5'-ACCCTCATAGAT GGGCACAG-3'. The primers of miR-132 (MQPS0000604) and U6 (MQPS0000002) were purchased from Guangzhou RiboBio Co., Ltd., (Guangzhou, China).

Western blot analysis. Western blot analysis of total protein content was performed as previously described (23). Briefly, protein was extracted from PASMCs and lung tissues in ice-cold radioimmunoprecipitation assay lysis buffer (P0013B, Beyotime Institute of Biotechnology, Shanghai, China) and quantified using Bicinchoninic Acid Protein Assay Reagent (Pierce; Thermo Fisher Scientific, Inc.). Protein lysate (40 μg/lane) was separated by 10% SDS-PAGE and blotted onto polyvinylidene difluoride membranes. The membranes were blocked with 5% non-fat milk for 1 h at room temperature and incubated with the following primary antibodies at 4˚C overnight: Rabbit anti-α-SMA monoclonal antibody (dilution, 1:1,000; A2547, Sigma-Aldrich; Merck KGaA); anti-SM22α polyclonal antibody (dilution, 1:1,000; HPA001925, Sigma-Aldrich; Merck KGaA); anti-PTEN polyclonal antibody (dilution, 1:1,000; D261095, Sangon Biotech Co., Ltd.); anti-p-PTEN polyclonal antibody (dilution, 1:1,000; D155023, Sangon Biotech Co., Ltd.); anti-α-tubulin monoclonal antibody (dilution, 1:5,000; A01410, GenScript, Piscataway, NJ, USA) and anti-β-actin monoclonal antibody (dilution, 1:5,000; A00702, GenScript). Following washing, membranes were incubated for 2 h at room temperature with horseradish peroxide-conjugated goat-anti-mouse (D110087) or goat-anti-rabbit (D110058) immunoglobulin G secondary antibodies (dilution, 1:6,000; Sangon Biotech Co., Ltd.). Finally, the protein expression levels were detected with an enhanced chemiluminescent substrate (cat. no. 32209, Thermo Fisher Scientific, Inc.) and recorded with ChemiDoc XRS+ system (Bio-Rad Laboratories, Inc., Hercules, CA, USA). The results were analyzed using ImageJ 1.52 software (National Institutes of Health, Bethesda, MD, USA).

Statistical analysis. The data are presented as the mean ± standard deviation of at least three independent experiments. Data analysis was conducted using GraphPad Prism 5.0 software (GraphPad Software, Inc., La Jolla, CA, USA). Comparisons between two groups were performed by a double-sided Student's t-test. A one-way analysis of variance test followed by a Student-Newman-Keuls post-hoc test was performed for multiple comparisons. $P<0.05$ was considered to indicate a statistically significant difference.

Results

miR-132 expression levels in MCT-induced PAH rats. To investigate whether miR-132 serves a role in PAH, the miR-132 expression levels in MCT-induced PAH rats were initially detected by RT-qPCR assays. The results indicated that the expression levels of miR-132 were upregulated in the rat lung tissues and PAs following 3 weeks of MCT exposure (Fig. 1A). The rats demonstrated increased RVSP and RV/(left ventricle + septum) ratios compared with that of the untreated group after 3 weeks of MCT exposure (Fig. 1B and C). Fig. 1D revealed that the medial thickness of the pulmonary artery was increased in the MCT-induced rats.

miR-132 expression levels in proliferating human PASMCs. Subsequently, the miR-132 expression levels in PASMCs that were stimulated by PDGF-BB were determined. As demonstrated in Fig. 1E, the miR-132 levels increased gradually following treatment of PASMCs with 20 ng/ml PDGF-BB from 2-48 h, indicating a time-dependent response. In addition, PDGF-BB resulted in a rapid increase of miR-132 expression levels in a dose-dependent manner (Fig. 1F).

Effects of miR-132 on human PASMC proliferation. To explore the role of miR-132 in PAH, its effects on the proliferation and cell cycle of PASMCs were detected using cell viability and flow cytometry assays. The results indicated that 20 nM miR-132 mimics significantly inhibited cell proliferation (Fig. 2A), while 50 nM miR-132 inhibitor promoted cell proliferation (Fig. 2B). Upregulation and downregulation of miR-132 following transfection of PASMCs with mimics and inhibitors, respectively, was demonstrated by RT-qPCR analysis (Fig. 2C). Furthermore, the results of the cell cycle assay indicated that the percentages of the cells that were present in the G2/M and S phases were decreased following miR-132 mimics (20 nM) treatment (Fig. 2D), indicating that the anti-proliferative effect of miR-132 was attributed to cell cycle arrest. In contrast to the miR-132 mimics, the miR-132 inhibitor (50 nM) decreased the percentage of the cells at the G_0/G_1-phase (Fig. 2E).

Effects of miR-132 on human PASMC migration. In addition to cell proliferation, the migration of PASMCs has been considered to be a contributor in the development of PAH. The results of the Transwell assay indicated that the overexpression of miR-132 significantly increased the migration of human PASMCs (Fig. 2F).

Effects of miR-132 on the human PASMC phenotype. To additionally validate the role of miR-132 in PAH, the phenotypic switch of PASMCs was investigated by determining the expression of mRNAs and proteins of smooth muscle cell (SMC) phenotypic markers following overexpression of miR-132. Overexpression of miR-132 in human PASMCs increased the levels of α-SMA, SM22α and CNN1 compared with those in the NC samples (Fig. 3A and B), indicating that miR-132 may be essential for maintaining the PASMC contractile phenotype.

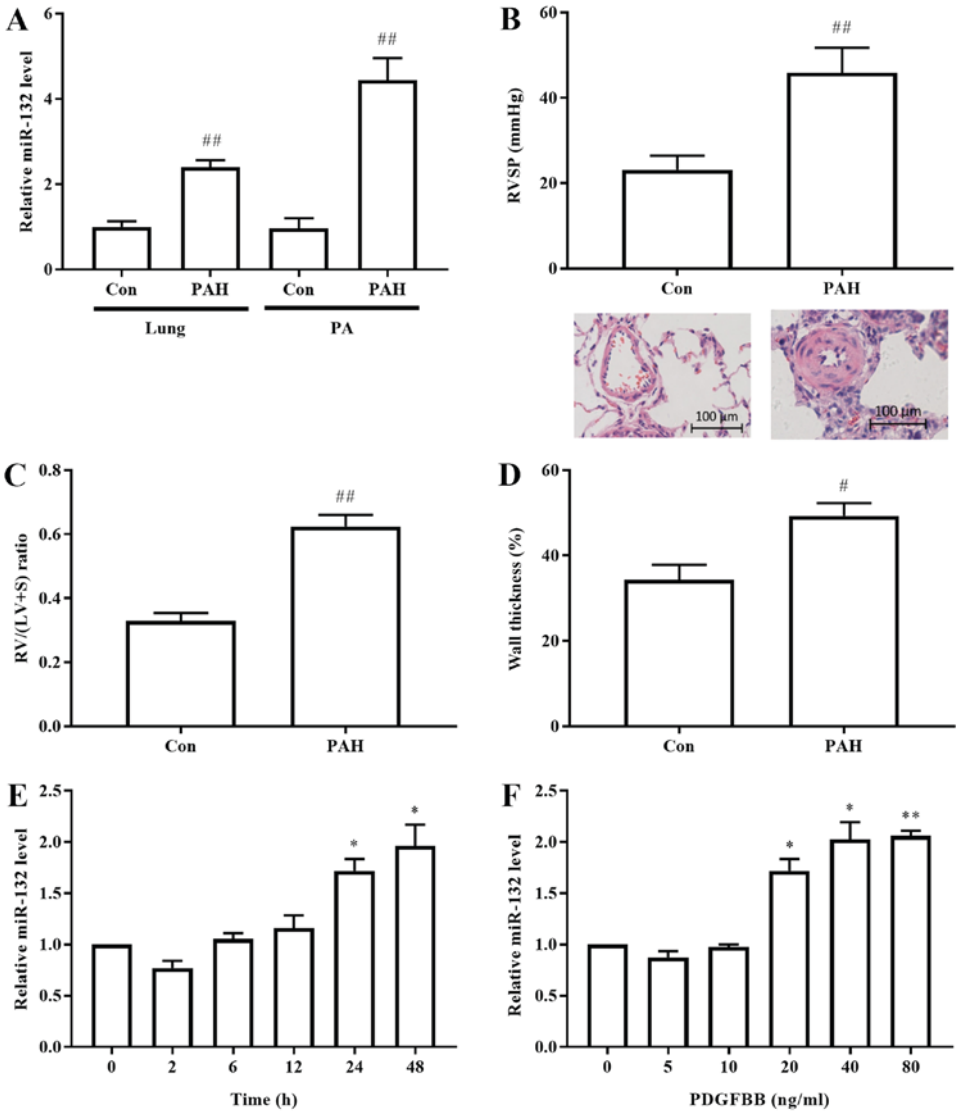

Figure 1. miR-132 expression is increased in MCT-induced PAH rats and PDGF-BB-treated PASMCs. (A) The levels of miR-132 were measured by reverse transcription polymerase chain reaction in lung tissues and PA from rats. (B) RVSP and (C) RV/(LV + S) ratios in the control and PAH rats were compared. (D) The degree of pulmonary arterial wall thickening in the rats was observed by hematoxylin and eosin staining. (E) PASMCs were treated with 20 ng/ml PDGF-BB for different incubation periods. (F) PASMCs were treated with various concentrations of PDGF-BB for 24 h and the miR-132 levels were assessed. Data are presented as the mean ± standard deviation (n=6). Scale bar, 100 μm. $^{\#}$P<0.05 and $^{\#\#}$P<0.01 vs. control. *P<0.05 and **P<0.01 vs. control without PDGF-BB treatment. miR, microRNA; con, control; PDGF-BB, platelet-derived growth factor BB; PAH, pulmonary arterial hypertension; PA, pulmonary artery; RVSP, right ventricular systolic pressure; RV, right ventricle/ventricular; LV, left ventricle/ventricular; S, septum.

PTEN is a direct target of miR-132. It has been demonstrated that PTEN is a direct target of miR-132 in vascular smooth muscle cells (VSMCs) (18). To examine the interaction between miR-132 and PTEN in PAH, the expression levels of PTEN were detected *in vivo* and *in vitro*. The results indicated that PTEN expression levels were decreased in MCT-induced PAH (Fig. 4A). Furthermore, it was identified that transfection of human PASMCs with miR-132 mimics downregulated the expression levels of PTEN significantly (Fig. 4B).

Discussion

PAH is a fatal disease without effective treatment and is primarily characterized by the excessive proliferation of PASMCs. Numerous studies have revealed that miRNAs serve a fundamental role in the pathogenesis of PAH by affecting the functions of PASMCs and pulmonary artery endothelial cells (24,25). In the present study, the role of miR-132 in PAH *in vivo* and in PASMCs *in vitro* was examined.

miR-132 is a highly conserved miRNA involved in the development of the central nervous and cardiovascular systems. Several studies have suggested that miR-132 expression is upregulated in certain cardiovascular diseases, including cardiac hypertrophy, hypertension and atherosclerosis (17,26,27). These studies demonstrated that miR-132 affected the proliferation and migration of cardiomyocytes, endothelial cells and VSMCs. Similarly, in the present study, miR-132 was highly expressed in PAH and its expression levels were markedly increased following PDGF-BB treatment, which indicated that miR-132 contributed to the development of PAH.

miR-132 has been demonstrated to regulate the function of vessel cells by different mechanisms of action. For example,

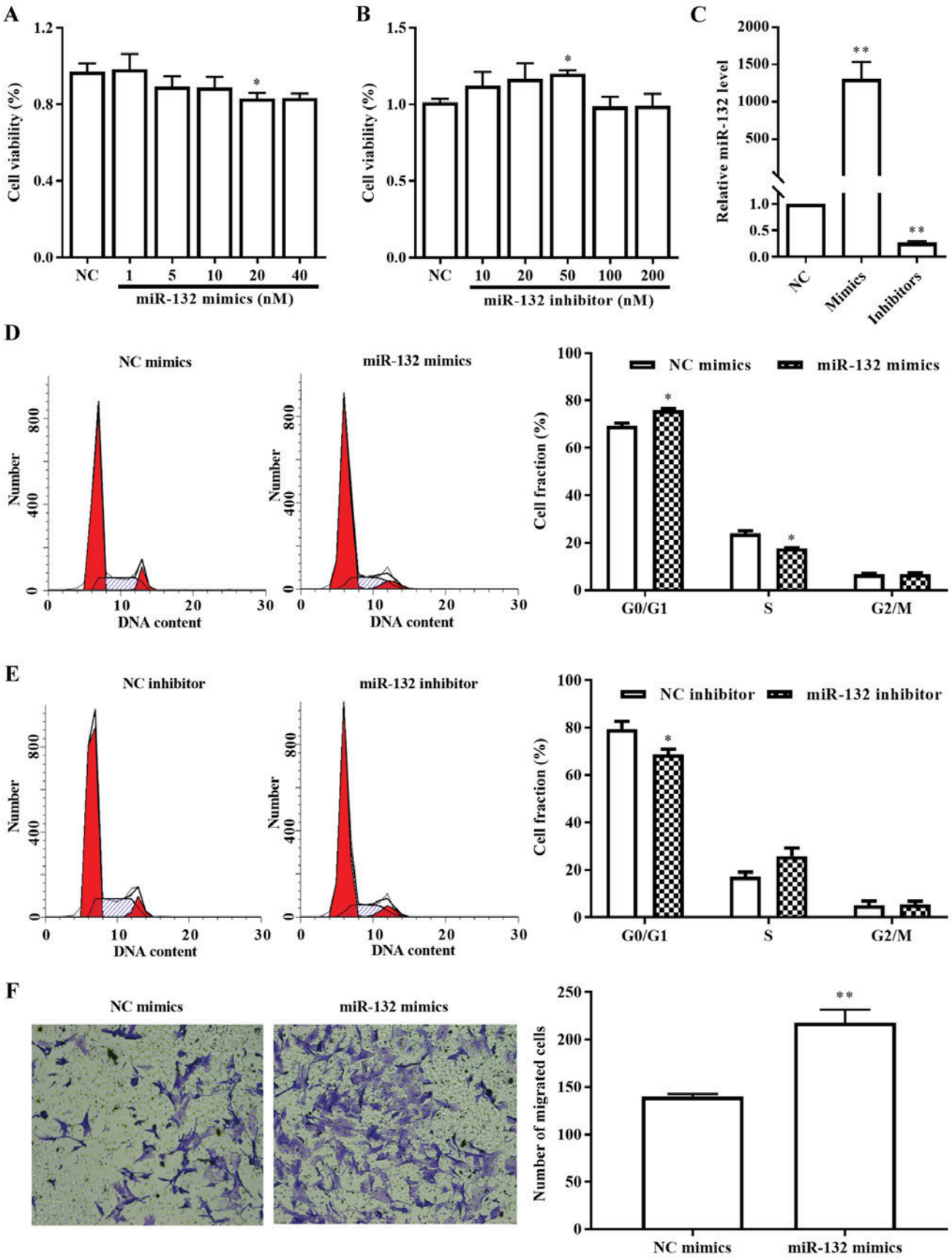

Figure 2. miR-132 inhibits PASMCs proliferation and promotes PASMCs migration. (A) Following treatment of PASMCs with various concentrations of miR-132 mimics for 72 h, the cell viability was detected using an MTS assay. (B) Following treatment of PASMCs with various concentrations of miR-132 inhibitors for 72 h, the cell viability was detected using an MTS assay. (C) Expression of miR-132 in PASMCs following transfection with 20 nM miR-132 mimics and 50 nM miR-132 inhibitor was determined by reverse transcription-quantitative polymerase chain reaction analysis. (D and E) The cell cycle of PASMCs transfected with 20 nM miR-132 mimics or 50 nM miR-132 inhibitor was determined by flow cytometry. (F) miR-132 mimics (20 nM) promoted PASMCs migration, as determined by the Transwell assay. Images are at magnification, x200. Data are presented as the mean ± standard deviation (n=3). *P<0.05 and **P<0.01 vs. NC. NC, negative control; miR, microRNA; PASMCs, pulmonary arterial smooth muscle cells.

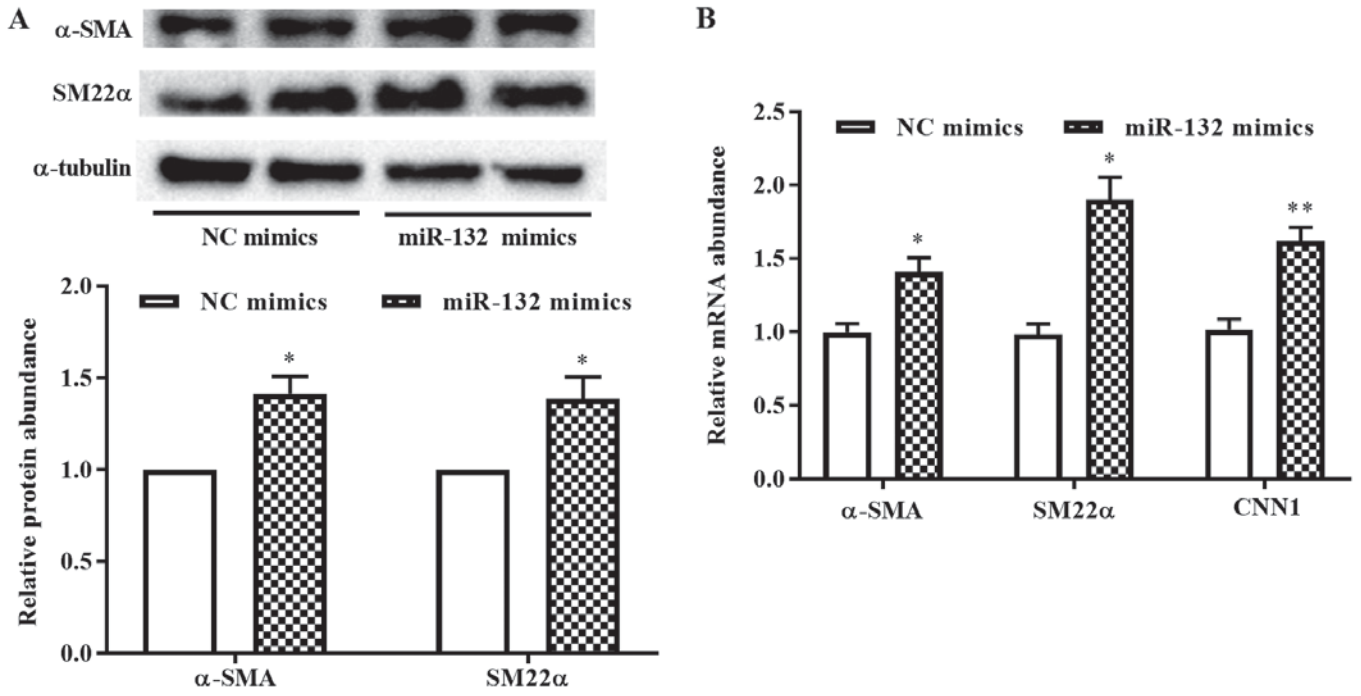

Figure 3. miR-132 induces the expression of smooth muscle cell contractile genes. (A) The relative protein levels of α-SMA and SM22α increased significantly following treatment of the cells with 20 nM miR-132 mimics. (B) The relative mRNA levels of α-SMA, *SM22α* and *CNN1* increased significantly following treatment of the cells with 20 nM miR-132 mimics. Data are presented as the mean ± standard deviation (n=3). *P<0.05 and **P<0.01 vs. NC. NC, negative control; miR, microRNA; α-SMA, α-smooth muscle actin; SM22α, transgelin; CNN1, calponin 1.

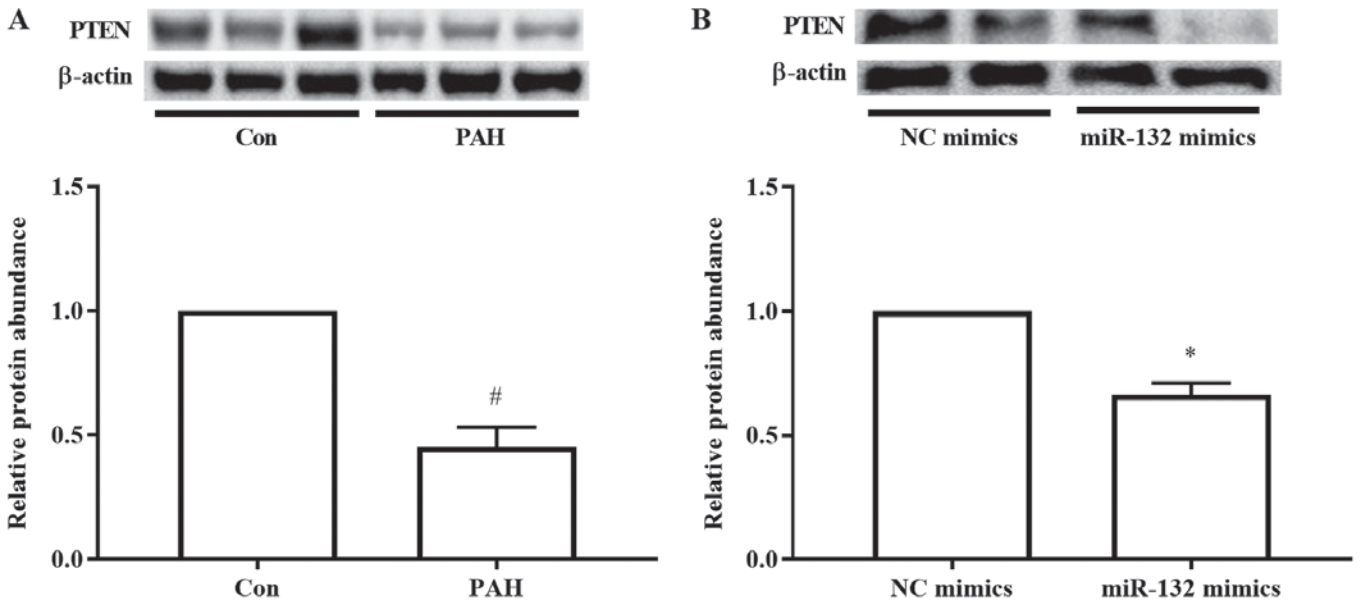

Figure 4. PTEN is a target of miR-132. (A) Downregulation of PTEN expression in the lung tissue of monocrotaline-induced PAH rats. (B) The relative protein levels of PTEN were significantly inhibited by treatment of 20 nM miR-132 mimics. Data are presented as the mean ± standard deviation (n=6). $^{\#}$P<0.05 vs. control. *P<0.05 vs. NC. NC, negative control; PTEN, phosphatase and tensin homolog deleted on chromosome 10; miR, microRNA; con, control; NC, negative control; PAH, pulmonary arterial hypertension.

miR-132 promoted the proliferation of endothelial cells via p120RasGAP (28) and inhibited the proliferation and migration of VSMCs (17) by targeting leucine-rich repeat flightless interacting protein 1. In contrast to these results, the present study revealed that miR-132 exerted multiple functions in PASMCs and served a complex role in the development of PAH, namely as an anti-proliferative factor in PASMCs and an aid to the maintenance of the contractile phenotype, while facilitating cell migration.

The major structural change observed during the development of PAH is the remodeling of small PAs, and typical vessel lesions that consist of neointima formation, medial thickening, adventitial fibrosis and angioproliferative plexiform lesions (29,30). These processes are accompanied with

proliferative and anti-apoptotic phenotypes of pulmonary endothelial cells, smooth muscle cells and fibroblasts (29,30). The data from the present study suggest that the pro-migrative effect of miR-132 contributed to the formation of plexiform lesions. However, its anti-proliferative and differentiation effects that were noted *in vivo* appeared to be contradictory to the results from the *in vitro* studies. The first possibility is that the proliferation of PASMCs is induced by other key factors including hypoxia, FGF and PDGF-BB. A second possible explanation is that the differentiation effect of miR-132 may facilitate the formation of SMCs and SMC-like cells. Taken collectively, these results provide novel evidence that miR-132 may be involved in the development of PAH and that it is detrimental to the development of vessel lesions. However, additional studies are required to ensure that the inhibition of miR-132 may prevent and reverse the progression of PAH.

The heterogeneous functions of miR-132 in SMCs are similar with those noted for the Krüppel-like factor 4 (KLF4), which is an additional key molecule involved in the regulation of SMC phenotypic switching and in the development of vascular diseases including PAH (31). Increased KLF4 levels in SMCs were demonstrated in injured vessels *in vivo* (32,33), and in response to PDGF-BB *in vitro* (32). KLF4 decreased SMC growth arrest by cellular tumor antigen p53-independent activation of cyclin-dependent kinase inhibitor 1, whereas it concomitantly induced SMC dedifferentiation via suppression of the expression of SMC-specific differentiation markers (32). This promoted SMC migration via binding to the collagen VIII alpha 1 promoter (32).

The present study explored the molecular mechanisms of miR-132 with regard to the regulation of PASMCs, with a focus on the miR-132-targeted gene PTEN (18), which is also downregulated in MCT-induced PAH (34). PTEN is well-known as a critical regulator of cell proliferation, apoptosis and migration (35). It has been demonstrated that inhibition of PTEN may attenuate PASMC proliferation and increase their migration through activation of RAC alpha serine/threonine-protein kinase (AKT) (35-37). Therefore, the present study aimed to investigate whether miR-132 may regulate PASMC function via the PTEN-AKT pathway. The data indicated that the expression of PTEN was decreased in the lung tissues of PAH rats and in miR-132-overexpressing PASMCs; however, the levels of phosphorylated AKT protein were also reduced (data not shown). PTEN is a suppressor of AKT phosphorylation and interacts with numerous downstream molecules (35). Thus, the targeting of PTEN by miR-132 may regulate the proliferation, migration and phenotype of PASMCs via the activation and/or suppression of other signaling pathways. The exact mechanism will be additionally explored in future studies.

In summary, the present study suggests that miR-132 served an important and pleiotropic role in modulating PASMC proliferation, migration and phenotypic switching by targeting PTEN. These data led to the identification of miR-132 as a potential target for the treatment of pulmonary vascular remodeling diseases.

Acknowledgements

Not applicable.

Funding

The present study was supported by the Scientific Research Fund of Hunan Provincial Education Department (grant no. 17B188).

Availability of data and materials

The datasets used and/or analyzed during the current study are available from the corresponding author on reasonable request.

Authors' contributions

ZZZ and WHW conceived and designed the study. QP, YHS and JXL performed the experiments. ZZZ wrote the paper. WW reviewed and edited the manuscript. All authors read and approved the manuscript.

Ethics approval and consent to participate

The present study was approved by the Ethics Committee of Hunan University of Medicine.

Patient consent for publication

Not applicable.

Competing interests

The authors declare that they have no competing interests.

References

1. Lau EMT, Giannoulatou E, Celermajer DS and Humbert M: Epidemiology and treatment of pulmonary arterial hypertension. Nat Rev Cardiol 14: 603-614, 2017.
2. Chen KH, Dasgupta A, Lin J, Potus F, Bonnet S, Iremonger J, Fu J, Mewburn J, Wu D, Dunham-Snary K, *et al*: Epigenetic dysregulation of the Drp1 binding partners MiD49 and MiD51 increases mitotic mitochondrial fission and promotes pulmonary arterial hypertension: Mechanistic and therapeutic implications. Circulation 138: 287-304, 2018.
3. Maron BA and Leopold JA: Emerging concepts in the molecular basis of pulmonary arterial hypertension: Part II: Neurohormonal signaling contributes to the pulmonary vascular and right ventricular pathophenotype of pulmonary arterial hypertension. Circulation 131: 2079-2091, 2015.
4. Ten Freyhaus H, Berghausen EM, Janssen W, Leuchs M, Zierden M, Murmann K, Klinke A, Vantler M, Caglayan E, Kramer T, *et al*: Genetic ablation of PDGF-Dependent signaling pathways abolishes vascular remodeling and experimental pulmonary hypertension. Arterioscler Thromb Vasc Biol 35: 1236-1245, 2015.
5. Tallquist M and Kazlauskas A: PDGF signaling in cells and mice. Cytokine Growth Factor Rev 15: 205-213, 2004.
6. Sysol JR, Natarajan V and Machado RF: PDGF induces SphK1 expression via Egr-1 to promote pulmonary artery smooth muscle cell proliferation. Am J Physiol Cell Physiol 310: C983-C992, 2016.
7. Chen J, Cui X, Li L, Qu J, Raj JU and Gou D: MiR-339 inhibits proliferation of pulmonary artery smooth muscle cell by targeting FGF signaling. Physiol Rep 5: e13441, 2017.
8. Picao-Osorio J, Johnston J, Landgraf M, Berni J and Alonso CR: MicroRNA-encoded behavior in drosophila. Science 350: 815-820, 2015.
9. Xiao T, Xie L, Huang M and Shen J: Differential expression of microRNA in the lungs of rats with pulmonary arterial hypertension. Mol Med Rep 15: 591-596, 2017.

10. Thenappan T, Ormiston ML, Ryan JJ and Archer SL: Pulmonary arterial hypertension: Pathogenesis and clinical management. BMJ 360: j5492, 2018.
11. Courboulin A, Paulin R, Giguère NJ, Saksouk N, Perreault T, Meloche J, Paquet ER, Biardel S, Provencher S, Côté J, *et al*: Role for miR-204 in human pulmonary arterial hypertension. J Exp Med 208: 535-548, 2011.
12. Sahoo S, Meijles DN, Al Ghouleh I, Tandon M, Cifuentes-Pagano E, Sembrat J, Rojas M, Goncharova E and Pagano PJ: MEF2C-MYOCD and Leiomodin1 suppression by miRNA-214 promotes smooth muscle cell phenotype switching in pulmonary arterial hypertension. PLoS One 11: e0153780, 2016.
13. Zhang WF, Xiong YW, Zhu TT, Xiong AZ, Bao HH and Cheng XS: MicroRNA let-7g inhibited hypoxia-induced proliferation of PASMCs via G0/G1 cell cycle arrest by targeting c-myc. Life Sci 170: 9-15, 2017.
14. Deng L, Baker AH and Bradshaw AC: MicroRNA delivery strategies to the lung in a model of pulmonary hypertension. Methods Mol Biol 1521: 325-338, 2017.
15. Bertero T, Cottrill K, Krauszman A, Lu Y, Annis S, Hale A, Bhat B, Waxman AB, Chau BN, Kuebler WM and Chan SY: The microRNA-130/301 family controls vasoconstriction in pulmonary hypertension. J Biol Chem 290: 2069-2085, 2015.
16. Liu HM, Jia Y, Zhang YX, Yan J, Liao N, Li XH and Tang Y: Dysregulation of miR-135a-5p promotes the development of rat pulmonary arterial hypertension in vivo and in vitro. Acta Pharmacol Sin: 2018.
17. Choe N, Kwon JS, Kim JR, Eom GH, Kim Y, Nam KI, Ahn Y, Kee HJ and Kook H: The microRNA miR-132 targets Lrrfip1 to block vascular smooth muscle cell proliferation and neointimal hyperplasia. Atherosclerosis 229: 348-355, 2013.
18. Jin W, Reddy MA, Chen Z, Putta S, Lanting L, Kato M, Park JT, Chandra M, Wang C, Tangirala RK and Natarajan R: Small RNA sequencing reveals microRNAs that modulate angiotensin II effects in vascular smooth muscle cells. J Biol Chem 287: 15672-15683, 2012.
19. Lai YJ, Hsu HH, Chang GJ, Lin SH, Chen WJ, Huang CC and Pang JS: Prostaglandin E1 attenuates pulmonary artery remodeling by activating phosphorylation of CREB and the PTEN signaling pathway. Sci Rep 7: 9974, 2017.
20. National Research Council: Guide for the care and use of laboratory animals. 8th edition. Washington (DC), National Academies Press (US), 2011.
21. Wu WH, Hu CP, Chen XP, Zhang WF, Li XW, Xiong XM and Li YJ: MicroRNA-130a mediates proliferation of vascular smooth muscle cells in hypertension. Am J Hypertens 24: 1087-1093, 2011.
22. Livak KJ and Schmittgen TD: Analysis of relative gene expression data using real-time quantitative PCR and the 2-ΔΔCt method. Methods 25: 402-408, 2001.
23. Zeng Z, Huang Q, Shu Z, Liu P, Chen S, Pan X, Zang L and Zhou S: Effects of short-chain acyl-CoA dehydrogenase on cardiomyocyte apoptosis. J Cell Mol Med 20: 1381-1391, 2016.
24. Bienertova-Vasku J, Novak J and Vasku A: MicroRNAs in pulmonary arterial hypertension: Pathogenesis, diagnosis and treatment. J Am Soc Hypertens 9: 221-234, 2015.
25. Leopold JA and Maron BA: Molecular mechanisms of pulmonary vascular remodeling in pulmonary arterial hypertension. Int J Mol Sci 17: E761, 2016.
26. Ucar A, Gupta SK, Fiedler J, Erikci E, Kardasinski M, Batkai S, Dangwal S, Kumarswamy R, Bang C, Holzmann A, *et al*: The miRNA-212/132 family regulates both cardiac hypertrophy and cardiomyocyte autophagy. Nat Commun 3: 1078, 2012.
27. Eskildsen TV, Jeppesen PL, Schneider M, Nossent AY, Sandberg MB, Hansen PB, Jensen CH, Hansen ML, Marcussen N, Rasmussen LM, *et al*: Angiotensin II regulates microRNA-132/-212 in hypertensive rats and humans. Int J Mol Sci 14: 11190-11207, 2013.
28. Anand S, Majeti BK, Acevedo LM, Murphy EA, Mukthavaram R, Scheppke L, Huang M, Shields DJ, Lindquist JN, Lapinski PE, *et al*: MicroRNA-132-mediated loss of p120RasGAP activates the endothelium to facilitate pathological angiogenesis. Nat Med 16: 909-914, 2010.
29. Ghataorhe P, Rhodes CJ, Harbaum L, Attard M, Wharton J and Wilkins MR: Pulmonary arterial hypertension-progress in understanding the disease and prioritizing strategies for drug development. J Intern Med 282: 129-141, 2017.
30. Lythgoe MP, Rhodes CJ, Ghataorhe P, Attard M, Wharton J and Wilkins MR: Why drugs fail in clinical trials in pulmonary arterial hypertension, and strategies to succeed in the future. Pharmacol Ther 164: 195-203, 2016.
31. Yoshida T and Hayashi M: Role of kruppel-like factor 4 and its binding proteins in vascular disease. J Atheroscler Thromb 21: 402-413, 2014.
32. Alexander MR and Owens GK: Epigenetic control of smooth muscle cell differentiation and phenotypic switching in vascular development and disease. Annu Rev Physiol 74: 13-40, 2012.
33. Liu Y, Sinha S, McDonald OG, Shang Y, Hoofnagle MH and Owens GK: Kruppel-like factor 4 abrogates myocardin-induced activation of smooth muscle gene expression. J Biol Chem 280: 9719-9727, 2005.
34. Ravi Y, Selvendiran K, Meduru S, Citro L, Naidu S, Khan M, Rivera BK, Sai-Sudhakar CB and Kuppusamy P: Dysregulation of PTEN in cardiopulmonary vascular remodeling induced by pulmonary hypertension. Cell Biochem Biophys 67: 363-372, 2013.
35. Lee YR, Chen M and Pandolfi PP: The functions and regulation of the PTEN tumour suppressor: New modes and prospects. Nat Rev Mol Cell Biol 19: 547-562, 2018.
36. Liu Y, Cao Y, Sun S, Zhu J, Gao S, Pang J, Zhu D and Sun Z: Transforming growth factor-beta1 upregulation triggers pulmonary artery smooth muscle cell proliferation and apoptosis imbalance in rats with hypoxic pulmonary hypertension via the PTEN/AKT pathways. Int J Biochem Cell Biol 77: 141-154, 2016.
37. Zhu B, Gong Y, Yan G, Wang D, Qiao Y, Wang Q, Liu B, Hou J, Li R and Tang C: Down-regulation of lncRNA MEG3 promotes hypoxia-induced human pulmonary artery smooth muscle cell proliferation and migration via repressing PTEN by sponging miR-21. Biochem Biophys Res Commun 495: 2125-2132, 2018.